A Closer Look at R_D and R_{D^*}

Debjyoti Bardhan[*][†]

Tata Institute of Fundamental Research
E-mail: debjyoti@theory.tifr.res.in

The measurement of R_D (R_{D^*}), the ratio of the branching fraction of $\overline{B} \to D\tau\bar{\nu}_\tau(\overline{B} \to D^*\tau\bar{\nu}_\tau)$ to that of $\overline{B} \to Dl\bar{\nu}_l(\overline{B} \to D^*l\bar{\nu}_l)$, shows 1.9σ (3.3σ) deviation from its Standard Model (SM) prediction. The combined deviation is at the level of 4σ according to the Heavy Flavour Averaging Group (HFAG). In the paper [1] , we perform an effective field theory analysis (at the dimension 6 level) of these potential New Physics (NP) signals assuming $SU(3)_C \times SU(2)_L \times U(1)_Y$ gauge invariance. We first show that, in general, R_D and R_{D^*} are theoretically independent observables and hence, their theoretical predictions are not correlated. We identify the operators that can explain the experimental measurements of R_D and R_{D^*} individually and also together. Motivated by the recent measurement of the τ polarisation in $\overline{B} \to D^*\tau\bar{\nu}_\tau$ decay, $P_\tau^{D^*}$ by the BELLE collaboration, we study the impact of a more precise measurement of $P_\tau^{D^*}$ (and a measurement of P_τ^D) on the various possible NP explanations. Furthermore, we show that the measurement of R_{D^*} in bins of q^2, the square of the invariant mass of the lepton neutrino system, along with the information on τ polarisation, can completely distinguish the various operator structures.

---

[*]Speaker.

[†]The speaker wishes to thank the co-authors on the paper for helping with the talk. Further, thanks is due to Prof. Amol Dighe and Prof. Gautam Bhattacharyya for valuable suggestions before the talk.

1. Introduction

The quantity $R_{D^{(*)}}$ is defined as the following ratio between two branching ratios:

$$R_{D^{(*)}} = \frac{\mathscr{B}(B \to D^{(*)} \tau \bar{\nu}_\tau)}{\mathscr{B}(B \to D^{(*)} l \bar{\nu}_l)} \tag{1.1}$$

where $l = e, \mu$. This quantity, being a ratio, is a 'clean' observable devoid of the systematic uncertainties that plague individual measurements of branching ratios. Experimental measurements of these two quantities - 0.397 ± 0.028 for R_D and 0.316 ± 0.019 for R_{D^*} [2] - don't match with the theoretical predictions from the Standard Model (SM) - 0.300 ± 0.011 for R_D and 0.254 ± 0.004 for R_{D^*}. This corresponds to deviations $1.9\,\sigma$ and $3.3\,\sigma$ significance for R_D and R_{D^*} respectively, while the discrepancy for the two taken together is quite large $\sim 4\sigma$ [1]. This might well be a signal for new physics and we perform a model-independent analysis of the process using six-dimensional operators; in this analysis, we assume that any NP only affects the third leptonic generation.

Besides R_D and R_{D^*}, we also consider the binned value of R_D and R_{D^*}, the polarisation of the final state τ lepton, P_τ^D and $P_\tau^{D^*}$ and the forward-backward asymmetry in the two processes, $\mathscr{A}_{FB}^D$ and $\mathscr{A}_{FB}^{D^*}$[2]. While a recent measurement of $P_\tau^{D^*}$ has been reported by BELLE for the first time (although with large errors) [4], none of the other quantities have been experimentally measured as yet. The definitions of the observables is given below:

$$\text{Binned } R_{D^{(*)}} : \quad R_{D^{(*)}}[q^2 \text{ bin}] = \frac{\mathscr{B}(B \to D^{(*)} \tau \bar{\nu}_\tau)[q^2 \text{ bin}]}{\mathscr{B}(B \to D^{(*)} l \bar{\nu}_l)[q^2 \text{ bin}]} \tag{1.2}$$

$$\text{Tau Polarisation} : \quad P_\tau^{D^{(*)}} = \frac{\Gamma_\tau^{D^{(*)}}(+) - \Gamma_\tau^{D^{(*)}}(-)}{\Gamma_\tau^{D^{(*)}}(+) + \Gamma_\tau^{D^{(*)}}(-)} \tag{1.3}$$

$$\text{FB Asymmetry} : \mathscr{A}_{FB}^{D^{(*)}} = \frac{\int_0^{\pi/2} \frac{d\Gamma_\tau^{D^{(*)}}}{d\theta} d\theta - \int_{\pi/2}^\pi \frac{d\Gamma_\tau^{D^{(*)}}}{d\theta} d\theta}{\int_0^{\pi/2} \frac{d\Gamma_\tau^{D^{(*)}}}{d\theta} d\theta - \int_{\pi/2}^\pi \frac{d\Gamma_\tau^{D^{(*)}}}{d\theta} d\theta} \tag{1.4}$$

The branching ratio can be written as

$$\frac{d^2 \mathscr{B}_\ell^{D^{(*)}}}{dq^2 d(\cos\theta)} = \mathscr{N} |p_{D^{(*)}}| \left(a_\ell^{D^{(*)}} + b_\ell^{D^{(*)}} \cos\theta + c_\ell^{D^{(*)}} \cos^2\theta \right) \tag{1.5}$$

where

$$\mathscr{N} = \frac{\tau_B G_F^2 |V_{cb}|^2 q^2}{256\pi^3 M_B^2} \left(1 - \frac{m_\ell^2}{q^2} \right)^2 \quad \text{and} \quad |p_{D^{(*)}}| = \frac{\sqrt{\lambda(M_B^2, M_{D^{(*)}}^2, q^2)}}{2M_B}$$

where $\lambda(a, b, c) = a^2 + b^2 + c^2 - 2(ab + bc + ca)$ and θ is the angle between the lepton and $D^{(*)}$-meson in the lepton-neutrino centre-of-mass frame.

The decay amplitude for the process can be factorised into two parts - the hadronic part an the leptonic part. The hadronic part of the decay amplitude cannot be calculated exactly and is parameterised using form factors. These form factors are calculated in some theoretical and numerical framework and, in this work, we choose to simply borrow those results.

---

[1]It is worth noting that even though the quoted results suggest a large deviation, a recent measurement of R_{D^*} by the BELLE collaboration [4] is consistent with the SM value, although the measurement is quite imprecise.

[2]In principle, various differential distributions are also sensitive to the different NP Lorentz structures, see e.g., [3].

2. Lagrangian and Operator Basis

The effective six-dimensional Lagrangian for $b \to c\ell\bar{\nu}_\ell$ we use for the analysis is given by:

$$\mathcal{O}_{\text{VL}}^{cb\ell} = [\bar{c}\gamma^\mu b][\bar{\ell}\gamma_\mu P_L \nu] \qquad\qquad \mathcal{O}_{\text{VR}}^{cb\ell} = [\bar{c}\gamma^\mu b][\bar{\ell}\gamma_\mu P_R \nu]$$
$$\mathcal{O}_{\text{AL}}^{cb\ell} = [\bar{c}\gamma^\mu \gamma_5 b][\bar{\ell}\gamma_\mu P_L \nu] \qquad\qquad \mathcal{O}_{\text{AR}}^{cb\ell} = [\bar{c}\gamma^\mu \gamma_5 b][\bar{\ell}\gamma_\mu P_R \nu]$$
$$\mathcal{O}_{\text{SL}}^{cb\ell} = [\bar{c} b][\bar{\ell} P_L \nu] \qquad\qquad\qquad \mathcal{O}_{\text{SR}}^{cb\ell} = [\bar{c} b][\bar{\ell} P_R \nu] \qquad (2.1)$$
$$\mathcal{O}_{\text{PL}}^{cb\ell} = [\bar{c}\gamma_5 b][[\bar{\ell} P_L \nu] \qquad\qquad \mathcal{O}_{\text{PR}}^{cb\ell} = [\bar{c}\gamma_5 b][[\bar{\ell} P_R \nu]$$
$$\mathcal{O}_{\text{TL}}^{cb\ell} = [\bar{c}\sigma^{\mu\nu} b][\bar{\ell}\sigma_{\mu\nu} P_L \nu] \qquad\quad \mathcal{O}_{\text{TR}}^{cb\ell} = [\bar{c}\sigma^{\mu\nu} b][\bar{\ell}\sigma_{\mu\nu} P_R \nu]$$

and the set of Wilson Coeffients (WCs) corresponding to these operators are defined at the renormalization scale $\mu = m_b$.

In the SM, we would have $C_{\text{VL}}^{cb\ell} = -C_{\text{AL}}^{cb\ell} = 1$. We wish to go beyond the SM, but we shall respect the full gauge invariance of the SM and consequently only consider the operators listed on the left in 2.1. Further, since it is difficult to build a microscopic model with tensor interaction, we neglect its contribution in this note.(For the study of tensor operators, refer to the Appendix of [1]).

3. Form Factors

3.1 For $B \to D$ decay

The non-zero hadronic matrix elements for $\bar{B} \to D$ transition (ignoring the tensor) are parameterized by

$$\langle D(p_D, M_D) | \bar{c}\gamma^\mu b | \bar{B}(p_B, M_B) \rangle = F_+(q^2)\Big[(p_B + p_D)^\mu - \frac{M_B^2 - M_D^2}{q^2}q^\mu\Big]$$
$$+ F_0(q^2)\frac{M_B^2 - M_D^2}{q^2}q^\mu$$
$$\langle D(p_D, M_D) | \bar{c} b | \bar{B}(p_B, M_B) \rangle = F_0(q^2)\frac{M_B^2 - M_D^2}{m_b - m_c} \qquad (3.1)$$

Calculations for the form factors $F_0(q^2)$ and $F_+(q^2)$ are known in a lattice framework [5]. The axial vector and the pseudoscalar matrix elements are zero from symmetry considerations and thus only the WCs C_{VL}^τ and C_{SL}^τ contribute to this decay.

3.2 For $B \to D^*$ decay

The non-zero hadronic matrix elements for $\bar{B} \to D^*$ transition are parametrised by

$$\langle D^*(p_{D^*}, M_{D^*}) | \bar{c}\gamma_\mu b | \bar{B}(p_B, M_B) \rangle = i\varepsilon_{\mu\nu\rho\sigma}\varepsilon^{\nu*}p_B^\rho p_{D^*}^\sigma \frac{2V(q^2)}{M_B + M_{D^*}}$$
$$\langle D^*(p_{D^*}, M_{D^*}) | \bar{c}\gamma_\mu \gamma_5 b | \bar{B}(p_B, M_B) \rangle = 2M_{D^*}\frac{\varepsilon^*.q}{q^2}q_\mu A_0(q^2) + (M_B + M_{D^*})\Big[\varepsilon_\mu^* - \frac{\varepsilon^*.q}{q^2}q_\mu\Big]A_1(q^2)$$
$$- \frac{\varepsilon^*.q}{M_B + M_{D^*}}\Big[(p_B + p_{D^*})_\mu - \frac{M_B^2 - M_{D^*}^2}{q^2}q_\mu\Big]A_2(q^2)$$
$$\langle D^*(p_{D^*}, M_{D^*}) | \bar{c}\gamma_5 b | \bar{B}(p_B, M_B) \rangle = -\varepsilon^*.q\frac{2M_{D^*}}{m_b + m_c}A_0(q^2) \qquad (3.2)$$

While no lattice calculations exist for the form factors in this case, they have been calculated in a Heavy Quark Effective Theory (HQET) framework [6] and we borrow those results. In this case, symmetry dictates that the scalar current is zero and thus there is no contribution to the decay width from C_{SL}^{τ}.

3.3 Independence of R_D and R_{D^*}

We see that while C_{VL}^{τ} and C_{SL}^{τ} contribute to the $B \to D$ decay process, C_{VL}^{τ}, C_{AL}^{τ} and C_{PL}^{τ} contribute to the other one. Thus, given the independence of the WCs, the two processes are independent of each other since they depend of different sets of WCs. In other words, R_D and R_{D^*} are theoretically independent measurements and allow for separate explanations.

4. Explaining R_D Alone

The quantities a_ℓ^D, b_ℓ^D and c_ℓ^D (in 1.5) can be calculated for a particular helicity of the final state lepton using a helicity amplitude approach. The complete expressions are given in [1] and it is not repeated here. Since only C_{VL}^{τ} and C_{SL}^{τ} are relevant, we can plot R_D as a variation of the two WCs and note the range of values for which it satisfies the experimental bounds. This is done in Fig. 1,
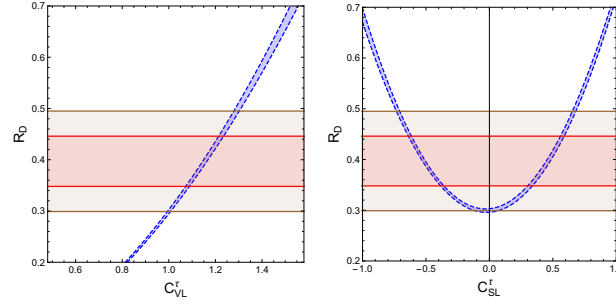

Figure 1: The dependence of R_D with respect to the variation of the WCs C_{VL}^{τ} (left) and C_{SL}^{τ} (right).

where the red (brown) band corresponds to the 1σ (2σ) value on the experimental measurement. We can use this range of the WCs to make a prediction of the value of the binned R_D, and for the
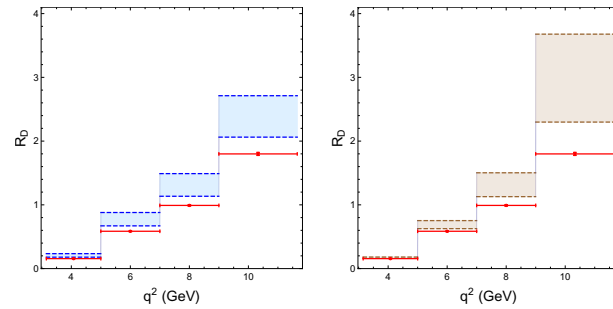

Figure 2: The binwise R_D for four q^2 bins. On the left, C_{VL}^{τ} is varied, while on the right, C_{SL}^{τ} is varied within their 1σ allowed ranges.

values of P_τ^D and $\mathscr{A}_{FB}^D$. These are shown in Fig. 2 and Fig. 3 respectively.

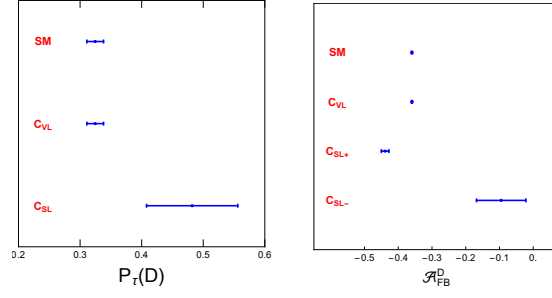**Figure 3:** Predictions for the polarisation fraction $P_\tau(D)$ (left) and $\mathscr{A}_{FB}^D$ (right)

5. Explaining R_{D^*} Alone

We can carry out a similar treatment for the case of $B \to D^*$ decay. In this case, three WCs - C_{VL}^τ, C_{AL}^τ and C_{PL}^τ - contribute. The plots of R_{D^*} as a function of the different WCs are given in Fig. 4 As before, the 1σ (2σ) bands are indicated by the red (brown) bands. The prediction for
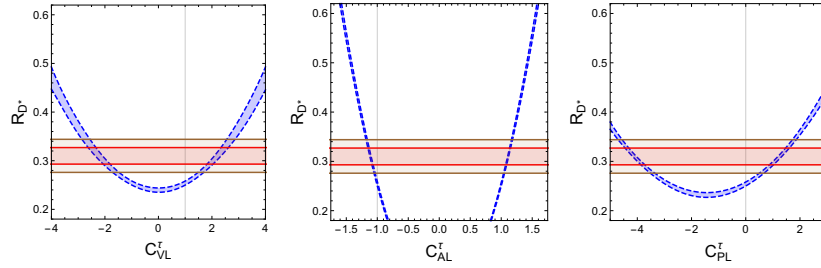

Figure 4: The dependence of R_{D^*} with respect to the variation of the WCs C_{VL}^τ (left), C_{AL}^τ (middle) and C_{PL}^τ (right). A thin vertical line shows the SM values of the WCs.
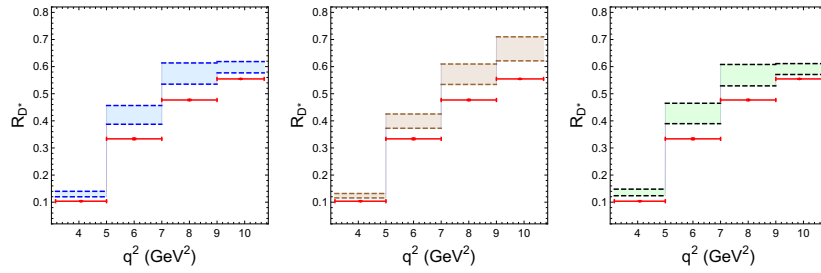

Figure 5: The binwise R_D^* for four q^2 bins. On the left, C_{VL}^τ is varied, in the middle C_{AL}^τ is varied, annd on the right, C_{PL}^τ is varied within their 1σ allowed ranges. The SM predictions are shown in red.

the binned R_{D^*} is given in Fig. 5. In this case, we do have a measurement of $P_\tau^{D^*}$, but it is quite imprecise. In the left plot of Fig. 6, the size of the errors indicated for the BELLE measurement is a projection with $20\ ab^{-1}$ data, which is expected to be collected by the year 2021; the central value
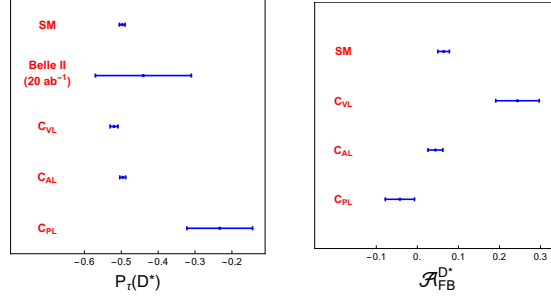
Figure 6: Predictions for the polarisation fraction $P_\tau(D^*)$ (left), $\mathscr{A}_{FB}^{D^*}$ (right). In the left plot, the Belle II 20 ab^{-1} projection is shown.

indicated is the current central value. As a matter of completion, we also plot the prediction for $\mathscr{A}_{FB}^{D^*}$ on the right of Fig. 6, although no measurement of this quantity exists as yet. We can combine
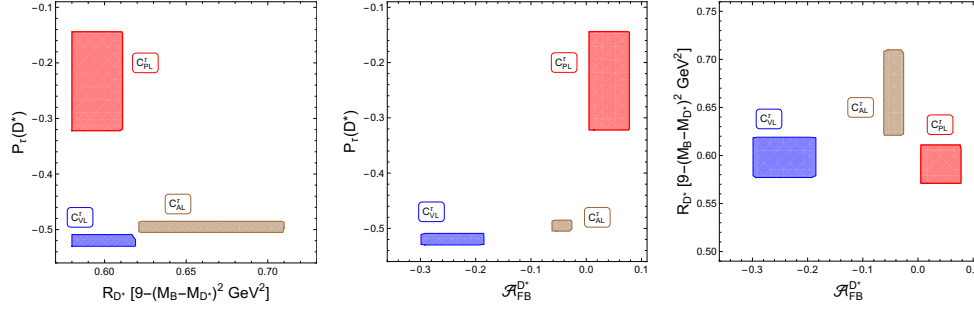

Figure 7: The predictions for $P_\tau^{D^*}$, R_{D^*} in the last bin and $\mathscr{A}_{FB}^{D^*}$ are shown in three different planes for the ranges of the three WCs C_{VL}^τ, C_{AL}^τ and C_{PL}^τ.

the predictions for the binned R_{D^*} restricted to the highest q^2 bin, $P_\tau^{D^*}$ and $\mathscr{A}_{FB}^{D^*}$ to construct three planes. When plotted in these three planes, the regions of the allowed values of the WCs all separate out nicely as shown in Fig. 7. A future measurement of any two of these three observables would help in restricting us to a particular region, thus limiting the scope of any NP model.

References

[1] D. Bardhan, P. Byakti and D. Ghosh, `1610.03038`

[2] HEAVY FLAVOR AVERAGING GROUP (HFAG) collaboration, Y. Amhis et al., `1412.7515`.

[3] A. Datta, M. Duraisamy and D. Ghosh, *Phys. Rev.* **D86**, 034027 (2012)

[4] A. Abdesselam et al., `1608.06391`.

[5] FERMILAB LATTICE, MILC collaboration, J. A. Bailey et al., *Phys. Rev.* **D89** (2014) 114504,

[6] I. Caprini, L. Lellouch and M. Neubert, *Nucl. Phys.* **B530** (1998) 153–181,